ELSEVIER

Bone Vol. 31, No. 5
November 2002:562–569

Mechanotransduction in Bone: Genetic Effects on Mechanosensitivity in Mice

A. G. ROBLING,[1] and C. H. TURNER[2]

[1]*Departments of Anatomy and Cell Biology and* [2]*Orthopaedic Surgery, Indiana University School of Medicine, Indianapolis, IN, USA*

Bone formation is enhanced by mechanical loading, but human exercise intervention studies have shown that the response to mechanical loading is variable, with some individuals exhibiting robust osteogenic responses while others respond modestly. Thus, mechanosensitivity — the ability of bone tissue to detect mechanical loads — could be under genetic control. We applied controlled mechanical loading to the ulnae of 20-week-old (adult) female mice derived from three different inbred strains (C3H/He, C57BL/6, and DBA/2), and measured the bone formation response with fluorochrome labels. Mechanical properties, including mechanical strain, second moments of area, and cortical bone material properties, were measured in a group of calibration animals not subjected to in vivo loading. The C3H/He mice were significantly less responsive to mechanical loading than the other two biological strains. Material properties (flexural elastic modulus, ultimate stress) were greatest in the C3H/He cortical tissue. Geometric and areal properties at the midshaft ulna were also greatest in the C3H/He mice. Based on the presumed role of osteocytes in strain detection, we measured osteocyte lacuna population densities in decalcified midshaft ulna sections. Osteocyte lacuna density was not related to mechanosensitivity. Our data suggest that bone mechanosensitivity has a significant genetic component. Identification of the genes that exert their influence on mechanosensitivity could ultimately lead to therapies that enhance bone mass and reduce fracture susceptibility. (Bone 31: 562–569; 2002)

Key Words: Bone adaptation; Mechanical loading; Mechanosensitivity; Bone modeling; Mouse ulna; Osteoporosis; Histomorphometry.

Introduction

Low bone mass is a major risk factor for osteoporotic fracture.[10,11,18] The amount of bone remaining in the female skeleton after the onset of menopause is strongly correlated with the peak amount of bone mass achieved much earlier in life.[11] These observations suggest that maximizing peak bone mass during the first two decades of life can have beneficial effects on fracture susceptibility and general skeletal fragility during the senescent years.

The accumulation of bone mass and the retardation of bone loss can be enhanced by environmental factors, such as mechanical loading (exercise) or calcium intake, but genetic studies have revealed that a large portion (60%–70%) of the variance in bone mineral density (BMD)—the best single predictor of bone fragility—is explained by heredity.[30–32] Consequently, understanding the signaling pathways targeted by the genes governing bone mass holds perhaps the greatest potential in affecting bone mass accumulation, and ultimately, fracture incidence. Obviously, the initial step in this strategy requires identifying the genes that exert their influence on BMD. However, the emerging picture in skeletal genetics indicates that bone mass and/or BMD is a complex trait, with contributions of varying potency from a number of genetic loci.[12,34]

Rodent models are particularly useful for studying the genetics of bone mass and other skeletal traits for a number of reasons, including: (i) there exists a wide range of skeletal phenotypic variation (e.g., BMD, strength) among different strains; (ii) the mammalian gestation/maturation period is short in rodents, allowing relatively quick creation of recombinant inbred and congenic strains; and (iii) gene mapping in mice and humans has revealed considerable homology in gene order between the two species, and many markers in the mouse genome have been mapped to the specific chromosomal positions in the human genome.

Of the available inbred mouse strains, three in particular have been studied extensively in skeletal genetics, C57BL/6, DBA/2, and C3H/He. The C57BL/6 strain is characterized by low BMD and large total cross-sectional area (CSA) in the midshaft femur; the C3H/He strain exhibits very high femoral BMD and a smaller femoral CSA than the C57BL/6 mice; and DBA/2 mice have moderately high femoral BMD and a very small midshaft femur CSA.[3,4] Linkage analysis conducted on intercrosses between the C57BL/6 and C3H/He strains, and on recombinant inbred strains generated from the C57BL/6 and DBA/2 cross, have revealed a number of quantitative trait loci (QTLs) affecting femoral BMD, femoral CSA, and whole body BMD.[5,20]

Mechanical loading of the skeleton during growth can substantially enhance periosteal bone apposition, and ultimately produce a diaphyseal cross section with enlarged area.[15,19] The C57BL/6 mice have a larger femoral CSA than the C3H/He and DBA/2 mice, yet the three strains exhibit similar body weights and activity levels. These observations led us to surmise that the mouse strain with greater femoral cross-sectional area (C57BL/6) might have a genetic predisposition for greater mechanosensitivity than mice with smaller cross sections (C3H/He and DBA/2). In other words, it is possible that bones that are

Address for correspondence and reprints: Dr. Alexander G. Robling, Department of Anatomy and Cell Biology, Indiana University School of Medicine, 635 Barnhill Drive, MS 5045, Indianapolis IN 46202. E-mail: arobling@anatomy.iupui.edu

8756-3282/02/$22.00
PII S8756-3282(02)00871-2

broader (greater CSA) became that way because they were more sensitive to routine mechanical loading signals. In support of this proposal, Kodama et al.[22] found that femora from C57BL/6 mice engaged in a high-intensity daily jumping protocol exhibited significantly greater periosteal mineral apposition rates, bone formation rates, and mechanical properties than femora from breed-matched nonjumping controls, but C3H/He mice subjected to the same treatment failed to show an increase in bone formation or strength as a result of the jumping protocol.

We undertook an investigation of in vivo skeletal mechanosensitivity in three biological strains of mice, by applying well-controlled dynamic loads to the ulnae and measuring the resulting osteogenic response. We hypothesized that the biological strain exhibiting the greatest CSA would exhibit the greatest osteogenic response to loading, and the biological strain exhibiting the least CSA would exhibit the least response to loading. We further sought to investigate the role of osteocyte lacuna population density in the observed differences in mechanosensitivity. The osteocyte network is commonly thought to be the primary mechanosensory apparatus in bone.[1,6,7,9,24] We further hypothesized that mouse strains exhibiting more mechanosensitive bones would have a greater population density of osteocyte lacunae than bones from mice that are less mechanosensitive.

Materials and Methods

Virgin female mice from each of the biological strains, C57BL/6 (n = 35), C3H/He (n = 30), and DBA/2 (n = 30), were purchased from Harlan, Inc. (Indianapolis, IN) at 13 weeks of age. The animals were housed at Indiana University's animal care facility for 7 weeks (acclimation period) before the experiment began. Standard mouse chow and water were provided ad libitum during the acclimation and loading periods. All procedures performed were in accordance with the Indiana University Animal Care and Use Committee guidelines.

In Situ Mechanical Properties of the Ulna and Radius

When the animals reached 20 weeks of age, five mice per biological strain were chosen at random, anesthetized, and killed by cervical dislocation. Immediately after killing, each animal was weighed and the left forearm was fixed between the cup-shaped platens of a miniature materials-testing machine (Vitrodyne V1000; Liveco, Inc., Burlington, VT), which has a force resolution of 0.05 N. The forearm was fixed in place using a small preload ($\backsim$0.1 N) that applied compression to the forearm through the olecranon and dorsal surface of the flexed wrist (**Figure 1**B). The forearms were loaded to failure in monotonic compression using a crosshead speed of 2 mm/sec, during which force and displacement measurements were collected every 0.01 sec. From the force vs. displacement curves, ultimate force (F_U; N), stiffness (S; N/mm), and work to ultimate force (U; mJ) were calculated.

In Situ Ulnar Strain During Dynamic Axial Loading

Immediately after the left forearm of each calibration animal was broken, the right arm was minimally dissected to expose the medial surface of the midshaft ulna. A single element strain gauge (Model EA-06-015DJ-120; Measurements Group, Inc., Raleigh, NC) was fixed to the exposed medial ulnar surface with cyanoacrylate (M-Bond 200; Measurements Group) at a point 3.35 mm distal to the brachialis insertion. Preliminary studies in our lab showed that this was the most reliable method for placing the gauge at the midshaft in the fleshed forearm, where the total length cannot be measured without significant dissection/disruption of the surrounding tissues. Once fitted with a strain gauge, the voltage was zeroed and the forearm was loaded in cyclic axial compression using an electromagnetic actuator with feedback control (Figure 1A). Using a 2 Hz haversine waveform, the forearms were loaded at 0.95, 1.40, 1.85, and 2.30 N, during which peak-to-peak voltage was measured on a digital oscilloscope. Voltage measurements were converted to strain using a calibration factor derived from measured and calculated (using beam theory) strains collected from an aluminum cantilever. Both mechanical testing in the left arm and strain gauging in the right arm were completed within 15 min after cervical dislocation. The right ulnae from the strain-gauged animals then were dissected free from the forelimb, with the strain gauge still attached, and fixed in refrigerated 10% neutral-buffered formalin. The right radius was dissected from the forelimb and stored in refrigerated 70% ethanol.

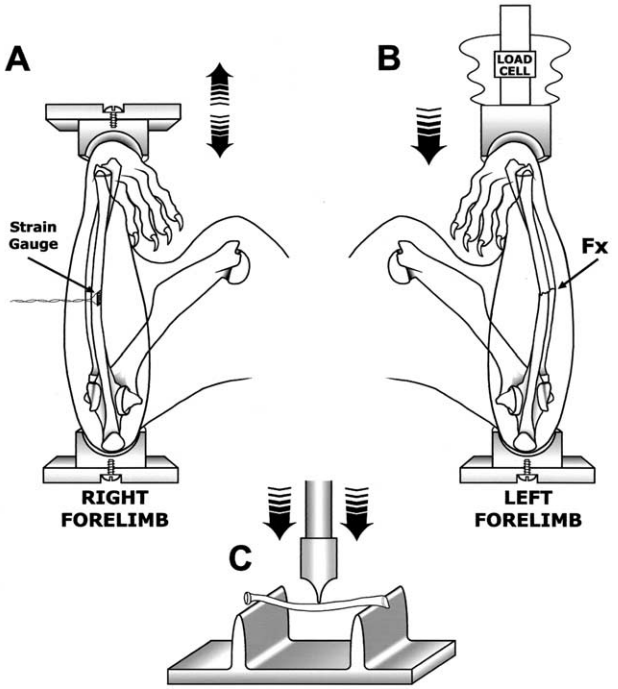

Figure 1. Immediately after killing, mice in the calibration groups (five per biological strain) were subjected to: (A) strain gauging of the right midshaft ulna in situ during dynamic loading (see Figure 4 for results); (B) mechanical testing of the left whole distal forearm in situ (see Figure 5 for results); and (C) mechanical testing (three-point bending) of the excised right radius (see Table 3 for results). The schematic in (A) is a scaled-down version of an ulna-loading model developed for rats.[35] The remaining animals in each inbred strain were loaded in vivo as illustrated in (A) (excluding the strain gauge) at 60 cycles/day for 3 days.

Bone Material Properties

We chose to use the radius for deriving material properties because of its long, straight, and cylindrical morphology, and because of its high aspect ratio. The right radii removed from the five calibration animals per biological strain were scanned in the transverse plane through the midshaft on a desktop μCT (μCT-20 Scanco Medical AG, Auenring, Switzerland) using 7 μm voxel size. Each midshaft radius slice was imported into SCIONIMAGE v4.0.2 for Windows (Scion Corp., Frederick, MD), wherein the second moment of area about the mediolateral axis (I_X; in mm^4) and the distance from the I_X neutral plane to the

Bone Vol. 31, No. 5
November 2002:562–569

outermost periosteal pixel on the caudal cortex (c_{PC}; mm) were calculated using standard and customized macros. The radii were then brought to room temperature slowly (~2 h) in a saline bath and broken in three-point bending. Each bone was positioned caudal side down across the lower supports of a miniature materials-testing machine (Vitrodyne V1000), which has a force resolution of 0.05 N (Figure 1B). The lower supports had a span of 8.7 mm. The radii were fixed in place using a ~0.1 N static preload before saline irrigation was initiated. Each radius was loaded to failure in three-point bending using a crosshead speed of 0.2 mm/sec, during which force and displacement measurements were collected every 0.01 sec. From the force vs. displacement curves, ultimate force (F_U; N) and stiffness (S; N/mm) were calculated. Flexural elastic modulus (E) and ultimate stress (σ_U) were calculated from the geometric and structural properties as follows:

$$E = S(L^3/48I_X) \quad (1)$$

$$\sigma_U = F_U(L\ c_{PC}/4I_X) \quad (2)$$

where L is the distance between lower supports.

Moment Arm Calculations for Ulnae

The strain-gauged ulnae removed from the five calibration animals per biological strain were scanned in the transverse plane through the center of the strain gauge (still attached at the midshaft) on a desktop μCT (μCT-20, Scanco Medical) using a 7 μm voxel size. The midshaft slices were imported into SCIONIMAGE, wherein I_{MIN} and the maximum section diameter in the I_{MIN} plane (Se.Dm; mm) were calculated. From the geometric measurements, mechanical strain recordings, and material properties derived from the radii of the respective biological strains, we calculated the average moment arm distance (d) for each biological strain during in situ loading:

$$d = \epsilon_{PM}E\ I_{MIN}/Fc_{PM} \quad (3)$$

where ϵ_{PM} is the strain measured on the medial periosteal surface per unit force (F), E is the mean flexural elastic modulus for each biological strain derived from the radius three-point bending tests, I_{MIN} approximates the second moment of area in the plane of bending during loading, F is the applied force, and c_{PM} is the distance from the I_{MIN} neutral plane to the outermost fiber on the medial periosteal surface. Because axial compression of the curved ulna produces a bending moment superimposed on axial compression, the I_{MIN} neutral plane is shifted laterally during axial loading from where it would be during pure bending. We estimated the position of the I_{MIN} neutral axis (and c_{PM}) during axial compression as 2/3Se.Dm, based on strain distributions measured in the rat ulna,[17] which exhibits similar morphology to the mouse ulna. Derivation of d allowed us to calculate strains on the medial periosteal surface from individual ulnar cross sections, based on their geometry (see later).

In Vivo Ulnar Loading

The remaining animals in each of the three biological strains were divided randomly into three groups for in vivo loading: low magnitude (36% of mean forearm F_U from calibration animals); medium magnitude (45% of mean F_U); or high magnitude (54% of mean F_U) loading (see Figure 5, arrows). Under ether-induced anesthesia, the right forearm of each mouse was loaded at 60 cycles/day for 3 consecutive days using a 2 Hz haversine waveform. The electromagnetic actuator used for strain-gauge measurements was used for in vivo loading. The left forearms were not loaded and served as an internal control for loading effects. All mice were allowed normal cage activity between loading bouts. Intraperitoneal injections of calcein (42 mg/kg body mass; Sigma Chemical Co., St. Louis, MO) were administered 4 and 8 days after the first loading day. All animals were killed 18 days after the first loading day.

Tissue Processing, Histomorphometry, and Ulnar Strain Calculations

Right and left ulnae were removed, cleaned of soft tissue, measured for total length, fixed in 10% neutral-buffered formalin for 48 h, dehydrated in graded alcohols, cleared in xylene, and embedded in methylmethacrylate (Aldrich Chemical Co., Inc., Milwaukee, WI). Using a diamond-embedded wire saw (Histosaw; Delaware Diamond Knives, Wilmington, DE), transverse thick sections (~70 μm) were removed from the ulnar midshaft. The wafers were ground to a final thickness of ~20 μm, and then mounted unstained on standard microscope slides.

One section per limb was read on a Nikon Optiphot fluorescence microscope (Nikon, Inc., Garden City, NJ) using the Bioquant digitizing system (R&M Biometrics, Nashville, TN). The following primary data were collected from the periosteal surface at ×425 magnification: total perimeter (B.Pm); single label perimeter (sL.Pm); double label perimeter (dL.Pm), measured along the first label; and double label area (dL.Ar). From these primary data, the following derived quantities were calculated: mineralizing surface (MS/BS = [1/2sL.Pm + dL.Pm]/B.Pm × 100; %); mineral apposition rate (MAR = dL.Ar/dL.Pm/4 days; μm/day); and bone formation rate (BFR/BS = MAR × MS/BS × 3.65; $\mu m^3/\mu m^2$ per year).[27] All of the derived quantities (measured from two-dimensional tissue sections) were converted into three-dimensional units using standard stereological techniques.[26] The same sections used for dynamic histomorphometry were evaluated under polarized white light to determine the microstructural organization of the newly formed bone tissue. To control for individual differences in systemic factors, left ulna (nonloaded control) values were subtracted from right ulna values; this procedure results in a new set of relative (r) values for each variable (e.g., rBFR/BS).

Each ulnar cross section used for fluorochrome histomorphometry was digitally captured through the microscope at ×250 magnification and imported into SCIONIMAGE, in which the following parameters were calculated from the sections using standard and customized macros: total area (Tt.Ar; mm^2); cortical area (Ct.Ar; mm^2); maximum second moment of area (I_{MAX}; mm^4); I_{MIN}; and Se.Dm. Mechanical strain was calculated for the medial periosteal surface of each histological section as follows

$$\epsilon_{PM} = F\ dc_{PM}/E\ I_{MIN} \quad (4)$$

where F is the force applied to the animal each day, d is the mean moment arm distance for each biological strain calculated from the strain-gauged animals (Equation 3), c_{PM} is 2/3Se.Dm, E is the mean flexural elastic modulus for each biological strain calculated from the radius three-point bending tests, and I_{MIN} approximates the second moment of area in the plane of bending.

The (right) strain-gauged ulnae from the calibration animals were decalcified in Decal I solution (Surgipath Medical Industries, Richmond, IL) after the strain gauges were removed. Each bone was embedded in paraffin and sectioned through the midshaft at 5 μm thickness using a Jung Histocut 820 microtome (Reichert-Jung, Inc., Germany). The sections were mounted on charged microscope slides, deparaffinized in xylene, dehydrated in graded alcohols, stained with hematoxylin-eosin, and coverslipped. On each section, the number of osteocyte lacunae

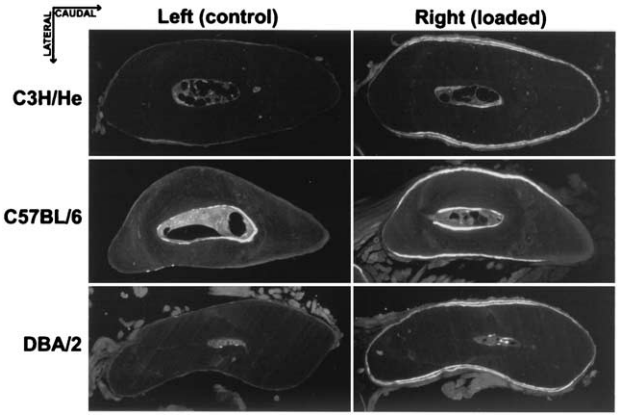

Figure 2. Mechanical loading of the right ulna activated the formerly quiescent medial and lateral periosteal surfaces in all three biological strains examined, as illustrated by the double calcein labeling. Bone formation induced by loading exhibited lamellar organization. Note the lack of response in the caudal and cranial periosteal surfaces, which straddle the neutral bending axis and are, consequently, subjected to very low strains. Note also the large total and cortical areas in the C3H/He cross section.

(Ot.Lc.N) was counted and the cortical area (Ct.Ar) was measured on a Nikon Optiphot research microscope under white light. Bioquant morphometry software was used to collect measurements from each section at ×250 magnification. From the two parameters, we calculated the population density of osteocyte lacunae (Ot.Lc.Dn) within the cortical bone (Ot.Lc.Dn = Ot.Lc.N/Ct.Ar).

Statistical Methods

Differences between bone formation parameters in the loaded (right) and nonloaded (left) ulnae were tested using Student's *t*-test for paired variates. Dose responses to different load magnitudes and mechanical strain within biological strains were tested for significance with least-squares regression. Differences in slope and x intercept (bone formation vs. mechanical strain, bone formation vs. peak load) among biological strains were tested for significance by analysis of covariance (ANCOVA). When ANCOVA detected significant differences among slopes, Tukey's HSD tests were performed to test pairwise comparisons of slopes and x intercepts (osteogenic threshold). For all tests, $\alpha = 0.05$.

Results

Fluorochrome-labeled sections revealed that most of the load-induced formation (bone between labels) was localized to the medial and lateral quadrants of the periosteal surface (**Figure 2**). All new bone formed during the experimental period was lamellar in organization. Mineralizing surface (MS/BS) and bone formation rate (BFR/BS) were significantly greater in the loaded ulnae compared with contralateral control ulnae for all biological strains, with the exception of the C57BL/6 low-load group (**Table 1**). In addition, MS/BS and BFR/BS were increased in a dose-dependent manner according to applied load magnitude. Mineral apposition rates (MAR) also showed a dose response with load magnitude in the right ulnae, but the mid-load C3H/He ulnae, the low-load C57BL/6 ulnae, and the low-load DBA/2 ulnae failed to show a statistical difference from the control ulnae values.

Relative (right minus left) bone formation rates (rBFR/BS) were closely associated with peak load magnitude ($p < 0.001$; **Figure 3**A). ANCOVA revealed statistically indistinguishable increases in rBFR/BS per unit of applied load ($p = 0.53$) among biological strains, but the x intercept was significantly ($p < 0.001$) lower in the DBA/2 (1.20 ± 0.2 N) mice compared with the C3H/He (1.85 ± 0.2 N) and C57BL/6 mice (1.85 ± 0.1 N). Relative BFR/BS was also closely associated with peak mechanical strain calculated for the midshaft ulna (Figure 3B). ANCOVA revealed significant differences among biological strains in the relation between mechanical strain and rBFR/BS. Tukey's HSD test indicated that the C3H/He mice exhibited significantly lower rBFR/BS per unit mechanical strain than the C57BL/6 and DBA/2 mice. In addition, the rBFR/BS x intercept for the C3H/He mice (2392 ± 242 με) was 29%–33% greater ($0.05 > p > 0.03$) than that for the C57BL/6 (1769 ± 130 με) and DBA/2 (1860 ± 168 με) mice.

The osteocyte lacuna population density (Ot.Lc.Dn) was significantly ($p < 0.05$) greater in the DBA/2 ulnae compared with the C57BL/6 ulnae (**Table 2**). Ot.Lc.Dn was intermediate in the C3H/He ulnae, but failed to reach a statistical difference vs. the other two biological strains.

Ulnar midshaft areal and geometric properties were greatest in the C3H/He mice, which exhibited 35% greater cortical area and 70% greater I_{MAX}, than the other two biological strains (Table 2). Total area in the C3H/He sections was 19% and 42% greater, and I_{MIN} was 11% and 136% greater, than in the C57BL/6 and DBA/2 sections, respectively. The C57BL/6 and DBA/2 mice exhibited similar (not statistically different) cortical area and I_{MAX} values, but total area and I_{MIN} were 19% and 112% greater, respectively, in the C57BL/6 ulnae compared to the DBA/2 ulnae.

Strain-gauge measurements from the medial surface of the right ulna revealed differences in ulnar compliance among the three biological strains of mice (**Figure 4**). Mechanical strain per unit load was least in the C57BL/6 mice, greatest in the DBA/2 mice, and intermediate in the C3H/He mice. The DBA/2 ulnae exhibited significantly greater compliance than C57BL/6 ulnae ($p = 0.03$), but the C57BL/6 vs. C3H/He and DBA/2 vs. C3H/He comparisons failed to reached statistical significance ($p = 0.09$ and 0.08, respectively).

Mechanical testing of the left forearm (ulna and radius) in situ revealed large differences in mechanical properties among the three biological strains (**Figure 5**). Ultimate force, stiffness, and work to ultimate force were greatest in the C3H/He mice, which exhibited 12%–24% ($0.0005 < p < 0.05$) greater F_U, S, and U values than the C57BL/6 mice. The C57BL/6 forearms exhibited 29%–43% ($0.0001 < p < 0.0016$) greater values than the DBA/2 forearms. All post hoc comparisons for each of the three mechanical variables reached statistical significance ($p < 0.05$).

The radius three-point bending tests showed significant differences in cortical bone material properties among biological strains (**Table 3**). The flexural elastic modulus was 20% greater ($p = 0.02$) in C3H/He mice compared to the C57BL/6 mice. DBA/2 mice exhibited an intermediate flexural modulus, which failed to reach statistical difference from the other two biological strains. Ultimate stress in the C3H/He mice was 13% greater than in the C57BL/6 mice and 15% greater than in the DBA/2 mice ($0.01 < p < 0.03$). No difference in ultimate stress was detected between C57BL/6 and DBA/2 cortical bone (Table 3).

At the start of the experiment (first loading day) and at time of killing, the C3H/He mice were heaviest, the DBA/2 mice were lightest, and the C57BL/6 mice were intermediate (Table 2). Neither the C57BL/6 nor the DBA/2 mice gained a significant amount of weight during the experiment, but the C3H/He mice were heavier at killing (0.5 g on average, $p = 0.005$) than they

Bone Vol. 31, No. 5
November 2002:562–569

Table 1. Periosteal bone formation measurements from the midshaft ulna in different biological strains of mice loaded at different peak magnitudes

Biological strain, load level, and side	n	MAR (μm/day) Mean ± SEM	MAR p value[a]	MS/BS (%) Mean ± SEM	MS/BS p value	BFR/BS ($\mu m^3/\mu m^2$ per year) Mean ± SEM	BFR/BS p value
C3H/He							
Low load (2.20 N)	9						
Right (loaded)		0.61 ± 0.07	$p < 0.05$	42.10 ± 6.59	$p < 0.001$	103.12 ± 24.70	$p < 0.01$
Left (control)		0.42 ± 0.06		15.53 ± 3.86		28.96 ± 10.10	
Mid load (2.75 N)	5						
Right (loaded)		0.90 ± 0.05	n.s.	67.57 ± 7.41	$p < 0.01$	221.65 ± 25.23	$p < 0.01$
Left (control)		0.69 ± 0.11		20.74 ± 3.93		53.78 ± 13.70	
High load (3.30 N)	7						
Right (loaded)		1.08 ± 0.11	$p < 0.05$	83.47 ± 3.77	$p < 0.001$	330.91 ± 43.15	$p < 0.01$
Left (control)		0.56 ± 0.11		16.78 ± 2.73		37.60 ± 10.73	
C57BL/6							
Low load (1.85 N)	11						
Right (loaded)		0.54 ± 0.09	n.s.	19.14 ± 2.60	n.s.	44.21 ± 12.18	n.s.
Left (control)		0.45 ± 0.07		17.78 ± 5.62		38.73 ± 17.50	
Mid load (2.30 N)	9						
Right (loaded)		0.75 ± 0.08	$p < 0.01$	40.63 ± 4.70	$p < 0.01$	116.04 ± 20.34	$p < 0.01$
Left (control)		0.33 ± 0.08		16.23 ± 4.39		28.54 ± 14.87	
High load (2.75 N)	10						
Right (loaded)		1.02 ± 0.10	$p < 0.001$	50.65 ± 3.12	$p < 0.001$	184.13 ± 16.97	$p < 0.001$
Left (control)		0.33 ± 0.05		15.10 ± 2.43		18.88 ± 4.98	
DBA/2							
Low load (1.55 N)	6						
Right (loaded)		0.67 ± 0.09	n.s.	46.04 ± 7.52	$p < 0.01$	120.91 ± 33.66	$p < 0.05$
Left (control)		0.39 ± 0.09		25.76 ± 5.33		40.56 ± 16.02	
Mid load (1.90 N)	8						
Right (loaded)		0.92 ± 0.11	$p < 0.01$	65.73 ± 2.02	$p < 0.01$	249.71 ± 55.16	$p < 0.01$
Left (control)		0.35 ± 0.05		23.19 ± 2.76		30.86 ± 6.82	
High load (2.25 N)	6						
Right (loaded)		1.07 ± 0.08	$p < 0.001$	72.45 ± 2.94	$p < 0.001$	284.53 ± 23.14	$p < 0.001$
Left (control)		0.30 ± 0.00		19.69 ± 4.36		21.56 ± 4.77	

See text for abbreviations.
[a]Probability associated with paired *t*-test between right and left values for each group; n.s. (not significant) indicates that the probability exceeds 0.05.

were on the first loading day. Paired *t*-tests within biological strains revealed that loading had no significant effect on ulnar length ($0.40 < p < 0.66$). However, the C3H/He ulnae were significantly longer than the C57BL/6 ulnae, which were significantly longer than the DBA/2 ulnae (Table 2).

Discussion

Our main objective in this study was to determine whether different biological strains of mice exhibit different degrees of sensitivity to the same mechanical stimulus. We hypothesized that mice exhibiting small ulnar cross-sectional areas would be less responsive to ulnar loading than mice with large ulnar cross-sectional areas. Our results indicate that C3H/He mice were clearly the least responsive to mechanical loading, yet they exhibited the largest ulnar cross section. Conversely, DBA/2 mice exhibited the smallest ulnar cross sections, but these mice were among the most sensitive to mechanical strain. The C57BL/6 mice exhibited a significantly larger ulnar cross section than the DBA/2 mice, yet these two biological strains exhibited almost exactly the same osteogenic response to loading (in terms of mechanical strain). Thus, it appears that bone size is not related to mechanosensitivity, at least among the inbred strains we examined.

The C3H/He mice appear to be least mechanosensitive in two key, independent parameters. First, the osteogenic threshold in the C3H/He mice (2392 με) was significantly greater than that in the C57BL/6 (1769 με) and DBA/2 (1860 με) mice. Mechanically induced bone formation is threshold driven, and bone formation signals will not be generated in the tissue unless a strain "setpoint" is surpassed.[14,16,23] The data show that, relative to the other two biological strains examined, C3H/He mice must generate more strain in their bones before an anabolic response is initiated. Second, once the (greater) osteogenic threshold was surpassed in the C3H/He ulna, the increase in bone formation per unit increase mechanical strain was significantly less than that in the other two biological strains. Thus, equal changes in suprathreshold strain did not result in equal changes in bone formation.

Our second objective was to determine the relation between osteocyte lacuna population density and mechanosensitivity. We hypothesized that the DBA/2 and C57BL/6 mice, in light of their greater mechanosensitivity, would have a greater population density of osteocyte lacunae than the C3H/He mice. However, the lacuna counts from the ulna midshaft sections were inconsistent with our hypothesis. The C3H/He and C57BL/6 mice exhibited statistically indistinguishable osteocyte lacuna densities, but the C3H/He mice were significantly less mechanosensitive than the C57BL/6 mice. In addition, the DBA/2 mice had significantly more lacunae per unit area than the C57BL/6 mice, but these two biological strains exhibited nearly identical mechanosensitivity. Thus, it appears that osteocyte lacuna population density is not related to mechanosensitivity in the three biological strains of mice tested.

Genetic effects on mechanosensitivity have been observed in

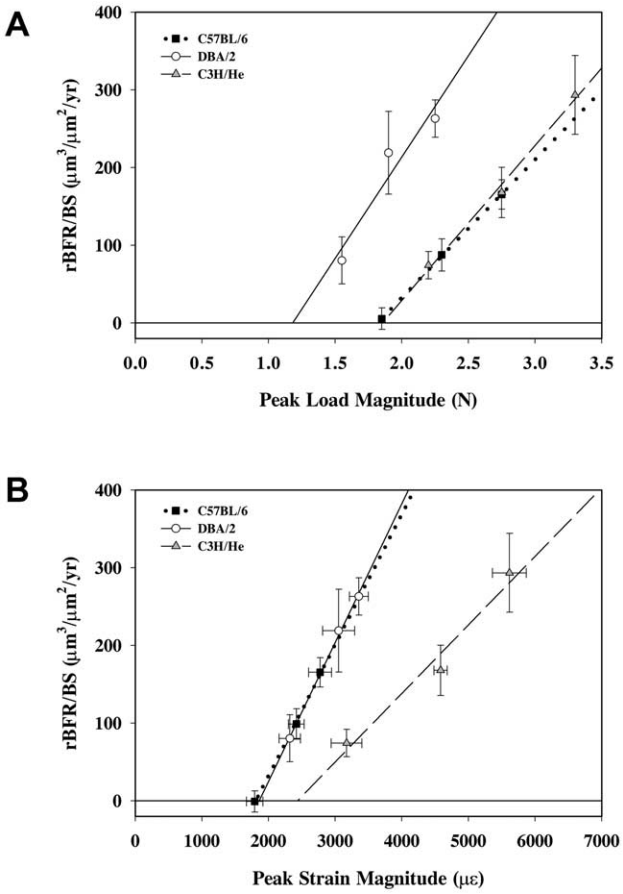

Figure 3. (A) Relative (right minus left) bone formation rate was significantly greater in the DBA/2 mice compared with the other two inbred strains when normalized to peak load magnitude. However, when rBFR/BS was normalized to peak mechanical strain (B), the DBA/2 and C57BL/6 mice exhibited identical (high) sensitivity, and the C3H/He mice showed both a higher osteogenic threshold and a lower rBFR/BS vs. strain slope (lower sensitivity). Error bars represent ±1 SE.

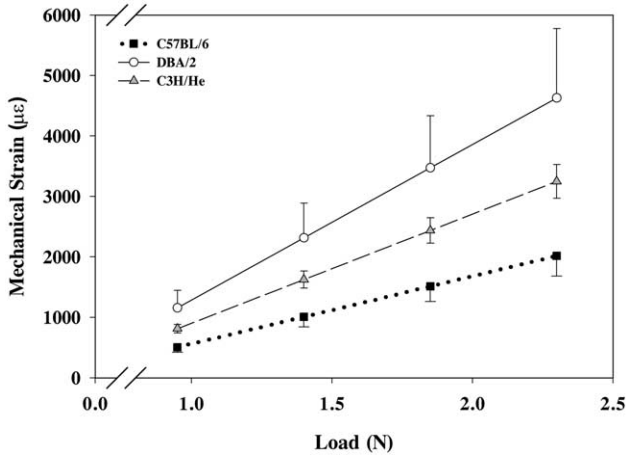

Figure 4. Strain measurements from the medial surface of the midshaft ulna were greatest in the DBA/2 mice, and significantly lower in the C57BL/6 mice. C3H/He exhibited a load vs. strain slope that was not significantly different from that derived for the other two biological strains. Error bars represent ±1 SE.

species other than mice. Pitsillides et al.[29] found that the tibiotarsi of newborn chicks specifically bred for high growth rate (meat-type) were significantly less sensitive to mechanical loading than tibiotarsi from chicks specifically bred for egg production (egg-type), in terms of early response mechanotransduction marker expression. Interestingly, the more responsive breed exhibited lower bone mass than the less responsive breed, a finding similar to ours for mice. Although several lines of evidence point to a genetic basis for mechanosensitivity, the genetic loci controlling this trait are not known. Mechanical loading studies in mice derived from genetic crosses of different biological strains offer the most streamlined approach to dissect out the genes playing major roles in mechanosensitivity.

Historically, the attainment of adult bone size, shape, and robusticity has been considered an epigenetic process,[13,36] and a wealth of experimental data support such a view.[8] The adaptive response seen in all three mouse strains in our experiments confirms the epigenetic adaptability of bone to mechanical stimulation. However, our experiments also indicate that the degree to which an individual (or mouse strain) responds to a mechanical stimulus appears to depend partly on genetics. These data challenge the purely epigenetic view of skeletal adaptation; different degrees of adaptation to the same stimulus are possible, and genetics probably plays a major role in determining such adaptability.

Among all three inbred strains, the bone formation response to loading comprised lamellar bone exclusively. Previous investigations of periosteal mechanoresponsiveness to extrinsic loading in C57BL/6 and C3H/He mice were based on woven bone responses, precluding a direct comparison to our results.[2,28] However, the lamellar bone formation response to loading on the tibial endocortical surface of C3H/He mice showed no response,[2] or suppressed bone formation,[28] in response to loading. Intrinsic loading experiments in C57BL/6 and C3H/He mice, in which the mice are trained to jump up to an

Table 2. Summary of body mass, ulnar bone lengths, midshaft ulnar areal properties, geometric properties, and osteocyte lacuna population densities in nonloaded ulnae from three biological strains of mice

Biological strain	Body-mass (g)		Ulna length (mm)[c]	Ct.Ar (mm^2)	Tt.Ar (mm^2)	I_{MAX} ($\times10^{-3}$; mm^4)	I_{MIN} ($\times10^{-3}$; mm^4)	Ot.Lc.Dn ($\times10^2$; #/mm^2)
	First loading	Time of killing						
C3H/He	24.6 ± 0.4	25.1 ± 0.4	14.2 ± 0.04	0.35 ± 0.01	0.37 ± 0.01	25.2 ± 1.7	5.10 ± 0.19	13.9 ± 0.7
C57BL/6	23.4 ± 0.2[a]	23.6 ± 0.3[a]	13.6 ± 0.02[a]	0.26 ± 0.01[a]	0.31 ± 0.01[a]	14.8 ± 0.9[a]	4.58 ± 0.19[a]	12.6 ± 1.2
DBA/2	22.0 ± 0.4[a,b]	21.9 ± 0.3[a,b]	13.4 ± 0.06[a,b]	0.26 ± 0.01[a]	0.26 ± 0.01[a,b]	14.9 ± 0.9[a]	2.16 ± 0.10[a,b]	16.3 ± 1.5[b]

See text for abbreviations.
[a]Significantly different from C3H/He values, based on Fisher's PLSD ($p < 0.05$).
[b]Significantly different from C57BL/6 values, based on Fisher's PLSD ($p < 0.05$).
[c]No significant differences were found between right (loaded) and left (control) bones for any of the biological strains: therefore, pooled (right and left) lengths values are reported.

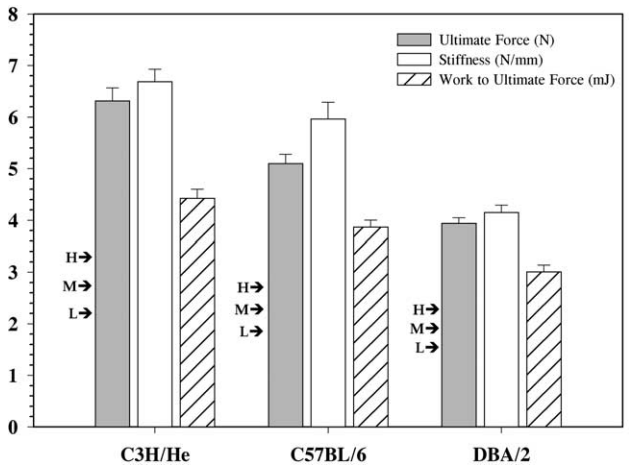

Figure 5. Ultimate force, stiffness, and work to ultimate force were greatest in the C3H/He distal forelimb (radius + ulna), least in the DBA/2 distal forelimb, and intermediate in the C57BL/6 distal forelimb. All pairwise comparisons between means were significant for all three mechanical parameters. The arrows to the left of the ultimate force bars illustrate the three load doses chosen per biological strain. H, high load (54% of F_U); M, mid-load (45% of F_U); L, low load (36% of F_U). Error bars represent ±1 SE.

elevated platform 20 times per day, revealed a robust osteogenic response in the C57BL/6 femoral midshaft, but the C3H/He femur showed no response to the same training. We were able to generate an osteogenic response, as well as a dose response, to loading in the C3H/He mice using the ulnar loading model, but like previous investigations we found that this biological strain was less responsive.

It is also of interest to note that, in addition to being less sensitive to enhanced loading conditions, the C3H/He mice are also less sensitive to reduced loading conditions. Kodama et al.[21] found that C3H/He mice lose significantly less bone in the tibia than C57BL/6 mice after sciatic neurectomy. These investigators later concluded that the marginal effects of disuse observed in the C3H/He mice were the result of an impaired ability to form osteoclasts and resorb bone.[25] These genetic effects on osteoclast biology do not explain the reduced responsiveness to loading that we observed, because the osteogenic response on the periosteum was entirely a modeling response, with no prior resorption activity observed.

The cross-sectional properties of the midshaft ulna (Tt.Ar, Ct.Ar, I_{MAX}, and I_{MIN}) were greatest in the C3H/He mice, least in the DBA/2 mice, and intermediate in the C57BL/6 mice. These trends (by biological strain) are similar to those reported for the midshaft femur, with the exception of Tt.Ar.[3] In the midshaft femur, C57BL/6 mice exhibited greater Tt.Ar than C3H/He mice, but the opposite relation was found in the midshaft ulna (see Table 2). The greater cortical and total areas in the C3H/He mice imparted significantly greater bending rigidity and second moments of area in the principal planes.

Table 3. Flexural elastic modulus (E) and ultimate stress (σ_U), derived from three-point bending tests of whole radii in three biological strains of mice

Biological strain	E (GPa)	σ_U (MPa)
C3H/He	15.9 ± 0.4	293 ± 1.3
C57BL/6	13.3 ± 0.7[a]	260 ± 11.8[a]
DBA/2	14.4 ± 0.8	254 ± 11.0[a]

[a]Significantly different from C3H/He values, based on Fisher's PLSD ($p < 0.05$).

The material properties derived from the radius tests were 1.6–5-fold greater than those reported in the literature from the femur, although the trends by biological strain were similar. Akhter et al.[3] reported flexural modulus in the range of 2.7–5.3 GPa and ultimate stress in the range of 110–180 MPa, whereas the values we found for the same parameters were in the range of 13.3–15.9 GPa and 254–293 MPa, respectively. These disparities are probably related to the specimen length-to-width aspect ratios associated with the respective tests. During a three-point bending test, the aspect ratio of length (distance between lower supports) to width (specimen diameter in the breaking plane) should be at least 20:1 to ensure a negligible shear component.[33] We chose to use the radius for deriving material properties because of its long, slender (∽0.65 mm diameter), almost perfectly cylindrical morphology, which enabled us to utilize a relatively large intersupport distance (8.7 mm) and reduce the shear component considerably. Although the aspect ratio associated with the radius tests (∽13:1) is lower than the recommended 20:1 ratio, it is roughly 2.5-fold greater than the ratio associated with tests conducted on the femur (∽5:1), which has a relatively thick (1.0–1.3 mm) cortex and requires a short lower support distance (5.0 mm) because of the bone's morphology.

The differences among biological strains in flexural elastic modulus (stiffness of the cortical material) corresponded well with volumetric BMD differences reported by Beamer et al.,[4] supporting the role of cortical bone mineralization in tissue stiffness. As expected, ultimate stress (the maximum amount of force per unit area endured by the material) followed the same trends as ultimate force for the whole forearm (radius + ulna) broken in situ. Thus, the mouse strain-related differences in material properties suggest that the matrix construction and/or mineralization process are partially under genetic control. It should be noted that we were unable to calculate material properties that require energy to failure (e.g., modulus of toughness), at least for the C57BL/6 radii, because the postyield displacement for this group exceeded the 2.5 mm total displacement we specified in the testing machine's control file. Consequently, unlike the C3H/He and DBA/2 radii, the C57BL/6 radii did not fail after 2.5 mm displacement, and remained unbroken (although plastically deformed) after completion of the test.

The main effect of loading on periosteal cell populations in all three biological strains appears to have been on both the rate of new bone apposition (MAR), and the number of active cells on the periosteal surface (MS/BS). A loading effect on MAR was not detected in the DBA/2 low-load group or in the C3H/He mid-load group. Table 1 shows that the lack of MAR response in the C3H/He mid-load group was the result of an unusually high control limb value, but the lack of MAR response in the DBA/2 low-load group was probably real. The lack of a loading effect on MS/BS and MAR, and consequently BFR/BS in the C57BL/6 low-load group, appears to have been the result of insufficient strain generated by the 1.85 N protocol.

In conclusion, significant differences in mechanosensitivity were found among the ulnae from three different biological strains of mice. In terms of peak mechanical strain, C3H/He mice appear to be less sensitive to mechanical loading than DBA/2 and C57BL/6 mice. The C3H/He mice exhibited a significantly greater osteogenic threshold, and significantly lower gain in bone per unit mechanical strain once the osteogenic threshold was exceeded, than DBA/2 and C57BL/6 mice. Differences in mechanosensitivity were not associated with differences in osteocyte lacuna population densities. Significant differences in cortical bone material properties and structural properties at the ulnar midshaft were also detected among

strains. The data suggest that bone's propensity to respond to mechanical loading is at least partially influenced by genes. Identifying the set of genes that exert their influence on mechanosensitivity has the potential to reveal target molecules and signaling pathways for pharmacological intervention, and ultimately to enhance bone mass and reduce fracture susceptibility.

Acknowledgments: The authors thank Mary Hooser and Diana Jacob for assistance with tissue processing. This work was supported by NIH Grants AR43730 and T32, AR07581.

References

1. Aarden, E. M., Burger, E. H., and Nijweide, P. J. Function of osteocytes in bone. J Cell Biochem 55:287–299; 1994.
2. Akhter, M. P., Cullen, D. M., Pedersen, E. A., Kimmel, D. B., and Recker, R. R. Bone response to in vivo mechanical loading in two breeds of mice. Calcif Tissue Int 63:442–449; 1998.
3. Akhter, M. P., Iwaniec, U. T., Covey, M. A., Cullen, D. M., Kimmel, D. B., and Recker, R. R. Genetic variations in bone density, histomorphometry, and strength in mice. Calcif Tissue Int 67:337–344; 2000.
4. Beamer, W. G., Donahue, L. R., Rosen, C. J., and Baylink, D. J. Genetic variability in adult bone density among inbred strains of mice. Bone 18:397–403; 1996.
5. Beamer, W. G., Shultz, K. L., Donahue, L. R., Churchill, G. A., Sen, S., Wergedal, J. R., Baylink, D. J., and Rosen, C. J. Quantitative trait loci for femoral and lumbar vertebral bone mineral density in C57BL/6J and C3H/HeJ inbred strains of mice. J Bone Miner Res 16:1195–206; 2001.
6. Burger, E. H. Mechanotransduction in bone—Role of the lacuno-canalicular network. FASEB J 13(Suppl.):S101–S112; 1999.
7. Burger, E. H., Klein-Nulend, J., van der Plas, A., and Nijweide, P. J. Function of osteocytes in bone — Their role in mechanotransduction. J Nutr 125:2020S–2023S; 1995.
8. Burr, D. B., Robling, A. G., and Turner, C. H. Effects of biomechanical stress on bones in animals. Bone 30:781–786; 2002.
9. Cowin, S. C. and Weinbaum, S. Strain amplification in the bone mechanosensory system. Am J Med Sci 316:184–188; 1998.
10. Cummings, S. R., Nevitt, M. C., Browner, W. S., Stone, K., Fox, K. M., Ensrud, K. E., Cauley, J., Black, D., and Vogt, T. M. Risk factors for hip fracture in white women. Study of Osteoporotic Fractures Research Group. N Engl J Med 332:767–773; 1995.
11. Duppe, H., Gardsell, P., Nilsson, B., and Johnell, O. A single bone density measurement can predict fractures over 25 years. Calcif Tissue Int 60:171–174; 1997.
12. Eisman, J. A. Genetics of osteoporosis. Endocrine Rev 20:788–804; 1999.
13. Frost, H. M. The Laws of Bone Structure. Springfield, IL: Thomas; 1964.
14. Frost, H. M. The mechanostat: A proposed pathogenic mechanism of osteoporoses and the bone mass effects of mechanical and nonmechanical agents. Bone Miner 2:73–85; 1987.
15. Haapasalo, H., Kontulainen, S., Sievanen, H., Kannus, P., Jarvinen, M., and Vuori, I. Exercise-induced bone gain is due to enlargement in bone size without a change in volumetric bone density: A peripheral quantitative computed tomography study of the upper arms of male tennis players. Bone 27:351–357; 2000.
16. Hsieh, Y.-F., Robling, A. G., Ambrosius, W. T., Burr, D. B., and Turner, C. H. Mechanical loading of diaphyseal bone in vivo: The strain threshold for an osteogenic response varies with location. J Bone Miner Res 16:2291–2297; 2001.
17. Hsieh, Y. F., Wang, T., and Turner, C. H. Viscoelastic response of the rat loading model: Implications for studies of strain-adaptive bone formation. Bone 25:379–382; 1999.
18. Hui, S. L., Slemenda, C. W., and Johnston, C. C. Jr. Baseline measurement of bone mass predicts fracture in white women. Ann Intern Med 111:355–361; 1989.
19. Kannus, P., Sievanen, H., and Vuori, I. Physical loading, exercise, and bone. Bone 18(Suppl.):1S–3S; 1996.
20. Klein, R. F., Mitchell, S. R., Phillips, T. J., Belknap, J. K., and Orwoll, E. S. Quantitative trait loci affecting peak bone mineral density in mice. J Bone Miner Res 13:1648–1656; 1998.
21. Kodama, Y., Dimai, H. P., Wergedal, J., Sheng, M., Malpe, R., Kutilek, S., Beamer, W., Donahue, L. R., Rosen, C., Baylink, D. J., and Farley, J. Cortical tibial bone volume in two strains of mice: Effects of sciatic neurectomy and genetic regulation of bone response to mechanical loading. Bone 25:183–190; 1999.
22. Kodama, Y., Umemura, Y., Nagasawa, S., Beamer, W. G., Donahue, L. R., Rosen, C. R., Baylink, D. J., and Farley, J. R. Exercise and mechanical loading increase periosteal bone formation and whole bone strength in C57BL/6J mice but not in C3H/HeJ mice. Calcif Tissue Int 66:298–306; 2000.
23. Lanyon, L. E. Functional strain in bone tissue as an objective, and controlling stimulus for adaptive bone remodelling. J Biomech 20:1083–1093; 1987.
24. Lanyon, L. E. Osteocytes, strain detection, bone modeling and remodeling. Calcif Tissue Int 53(Suppl. 1):S102–S107; 1993.
25. Linkhart, T. A., Linkhart, S. G., Kodama, Y., Farley, J. R., Dimai, H. P., Wright, K. R., Wergedal, J. E., Sheng, M., Beamer, W. G., Donahue, L. R., Rosen, C. J., and Baylink, D. J. Osteoclast formation in bone marrow cultures from two inbred strains of mice with different bone densities. J Bone Miner Res 14:39–46; 1999.
26. Parfitt, A. M. Stereologic basis of bone histomorphometry: Theory of quantitative microscopy and reconstruction of the third dimension. In: Recker, R. R., ed. Bone Histomorphometry: Techniques and Interpretation. Boca Raton, FL: CRC; 53–88; 1983.
27. Parfitt, A. M., Drezner, M. K., Glorieux, F. H., Kanis, J. A., Malluche, H., Meunier, P. J., Ott, S. M., and Recker, R. R. Bone histomorphometry: Standardization of nomenclature, symbols, and units. Report of the ASBMR Histomorphometry Nomenclature Committee. J Bone Miner Res 2:595–610; 1987.
28. Pedersen, E. A., Akhter, M. P., Cullen, D. M., Kimmel, D. B., and Recker, R. R. Bone response to in vivo mechanical loading in C3H/HeJ mice. Calcif Tissue Int 65:41–46; 1999.
29. Pitsillides, A. A., Rawlinson, S. C., Mosley, J. R., and Lanyon, L. E. Bone's early responses to mechanical loading differ in distinct genetic strains of chick: Selection for enhanced growth reduces skeletal adaptability. J Bone Miner Res 14:980–987; 1999.
30. Pocock, N. A., Eisman, J. A., Hopper, J. L., Yeates, M. G., Sambrook, P. N., and Eberl, S. Genetic determinants of bone mass in adults. A twin study. J Clin Invest 80:706–710; 1987.
31. Seeman, E., Hopper, J. L., Bach, L. A., Cooper, M. E., Parkinson, E., McKay, J., and Jerums, G. Reduced bone mass in daughters of women with osteoporosis. N Engl J Med 320:554–558; 1989.
32. Slemenda, C. W., Christian, J. C., Williams, C. J., Norton, J. A., and Johnston, C. C. Jr. Genetic determinants of bone mass in adult women: A reevaluation of the twin model and the potential importance of gene interaction on heritability estimates. J Bone Miner Res 6:561–567; 1991.
33. Spatz, H. C., O'Leary, E. J., and Vincent, J. F. Young's moduli and shear moduli in cortical bone. Proc R Soc Lond B Biol Sci 263:287–294; 1996.
34. Stewart, T. L. and Ralston, S. H. Role of genetic factors in the pathogenesis of osteoporosis. J Endocrinol 166:235–245; 2000.
35. Torrance, A. G., Mosley, J. R., Suswillo, R. F., and Lanyon, L. E. Noninvasive loading of the rat ulna in vivo induces a strain-related modeling response uncomplicated by trauma or periosteal pressure. Calcif Tissue Int 54:241–247; 1994.
36. Wolff, J. The Law of Bone Remodelling. New York: Springer; 1986.

Date Received: March 4, 2002
Date Revised: June 10, 2002
Date Accepted: July 11, 2002